In vitro assay of cytoskeleton nanomechanics as a tool for screening potential anticancer effects of natural plant extract, tubeimoside I on human hepatoma (HepG2) cells

ZHAO HongBo[1,2†], WANG YaShu[3†], JIANG XueMei[2], SHI XiaoHao[1], ZHONG HongZhe[4], WANG YaJie[5], CHEN Jun[2] & DENG LinHong[1,2*]

[1] *Institute of Biomedical Engineering & Health Sciences, Changzhou University, Changzhou 213164, China;*

[2] *Key Laboratory of Biorheological Science and Technology, Ministry of Education, and Bioengineering College, Chongqing University, Chongqing 400044, China;*

[3] *Xinjiang Provincial Corps Hospital, Chinese People's Armed Police Forces, Urumqi 830002, China;*

[4] *Liaoning Provincial Blood Center, Shenyang 110044, China;*

[5] *The 324th Hospital of the Chinese People's Liberation Army, Chongqing 400020, China*

Cytoskeleton nanomechanics characterizes cancer cell's physical behaviors such as how it spread and invade. For anticancer drug, cytoskeleton nanomechanics may be a target to inhibit invasiveness and metastasis of cancer cells. Therefore, *in vitro* assay of cytoskeleton nanomechanics may be used to evaluate the effects of potential anticancer drug on various cancer types. Here, we investigated the effects of tubeimoside I (TBMS I) on human hepatoma (HepG2) cells by using optical magnetic twisting cytometry, a well-established technique for measuring nanomechanics of the F-actin cytoskeleton. TBMS I is a natural compound extracted from a traditional Chinese herbal medicine, and is reported with antitumor effect. In this study, we demonstrated that the cytoskeleton stiffness (G') of HepG2 cells was affected by TBMS I. G' exhibited a typical power law with respect to the loading frequency (f), i.e. $G \sim f^{\alpha}$. The magnitude of G' and the value of exponent (α) of the HepG2 cells decreased consistently with the increase of concentration for TBMS I exposure. In addition, the HepG2 cells responded to TBMS I much faster than the normal liver (L-02) cells. Such alteration of cytoskeleton nanomechanics induced by TBMS I was reported for the first time, which was further corroborated by assays of F-actin cytoskeleton structure and cell migration. Taken together, these results suggest that *in vitro* assay of cytoskeleton nanomechanics may have a great potential as an additional tool in screening of anticancer drug candidates.

HepG2 cells, F-actin cytoskeleton, nanomechanics, tubeimoside I, anticancer drug screening

Citation: Zhao H B, Wang Y S, Jiang X M, et al. *In vitro* assay of cytoskeleton nanomechanics as a tool for screening potential anticancer effects of natural plant extract, tubeimoside I on human hepatoma (HepG2) cells. Chin Sci Bull, 2013, 58: 2576–2583, doi: 10.1007/s11434-013-5757-7

In the last two decades, tremendous advancements in both nanotechnology and photonic/optic technology have led to increasingly more innovative and versatile methods and devices for detection and measurement of physical and/or chemical events at micro/nanometer scales. One particularly important application of these developments is to the study of cytoskeleton nanomechanics that quantifies and characterizes nanoscale mechanical properties/behaviors of the cytoskeleton in living cells. Because of the unprecedented spatial and temporal resolution of cytoskeleton nanomechanics, it has been widely recognized as the cutting edge tool in elucidating previously elusive mechanisms of intricate biological processes in health and disease such as cell migration, cancer cell metastasis, and tissue morphogenesis. Less well recognized, however, is the potential for cyto-

---

†These authors contributed equally to this work.
*Corresponding author (email: dlh@cczu.edu.cn)

skeleton nanomechanics as a novel tool to investigate pharmacological action of drug in the living cell. For example, change of cancer cell stiffness, a key feature of its cytoskeleton nanomechanics, can not only provide hints of the cancer's malignancy and invasiveness, but may also be used to quantify the effect of a potential anticancer drug on the cancer cell's behavior. Due to nanomechanical transduction of biochemical reactions, characterization of cytoskeleton nanomechanics allows sensitive, label-free, direct, real-time and multiplexed detection of molecules as well as specific investigations of molecular interactions and conformational changes within the living cells. Therefore, the approach of cytoskeleton nanomechanics can be a very valuable addition in the portfolio of drug screening techniques.

Here, we investigate the effects of tubeimoside I, a natural plant extract and potential anticancer agent, on the cytoskeleton nanomechanics of human hepatoma (HepG2) cells in culture. Tubeimoside (TBMS), or the tuber of *Bolbostemma paniculatum* (Maxim.) Franquet (Cucurbitaceae) is a herb that has long been used in traditional Chinese medicine, and was listed in Supplement to the Compendium of Materia Medica published in early 1765 [1]. TBMS is most widely used for treatment of illness such as inflammation and snake venoms, but it has also been reported to show potent anti-tumor activity [2]. Such anti-tumor activity in part motivated the successful isolation of TBMS I, a triterpenoid saponin with chemical structure as shown in Figure 1 [3,4]. And subsequent studies confirmed that TBMS I can indeed inhibit growth of cultured cancer cells of several human cancer cell lines including human promyelocytic leukemia (HL-60) [5], nasopharyngeal carcinoma CNE-2Z cell line (CNE-2Z) [6] and HeLa cells [7],
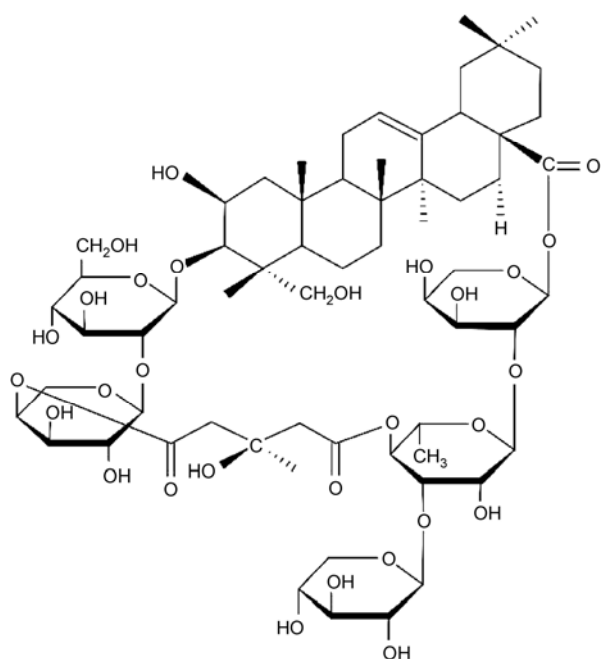
These studies appear to suggest that TBMS I may be a potential candidate as a novel anti-tumor drug.

Previous studies have identified that TBMS I targets cancer cells by altering the functions of microtubule [8], mitochondria [9] and endoplasmic reticulum [10], mostly through biochemical signaling pathways. It has, however, not been studied whether and how TBMS I may affect the cytoskeleton nanomechanics of cancer cells. Therefore, we evaluated TBMS I for its target on the nanomechanics of HepG2 cells, a well characterized human liver cancer cell type. We used optical magnetic twisting cytometry (OMTC), a well established method for cell nanomechanics, to measure the F-actin cytoskeleton stiffness of HepG2 cells in the absence or presence of TBMS I. In addition, we used Transwell® assay to examine the migration, and fluorescent microscopy to examine the F-actin cytoskeleton structure of HepG2 cells when exposed to TBMS I.

Furthermore, the effects of TBMS I on HepG2 cells were compared to those on normal liver cells. Thus, we found that the cytoskeleton of HepG2 cells responded to TBMS I with depolymerization and reduced stiffness of the F-actin cytoskeleton, together with reduced migration rate. All these responses were greater and probably faster in HepG2 cells than in normal liver cells, suggesting that TBMS I may be a drug candidate to specifically target cytoskeleton nanomechanics of HepG2 cells.

1 Methods and materials

1.1 Cell culture

Human hepatocellular carcinoma cell line (HepG2) and normal liver cell line (L-02) were obtained from American Type Culture Center (ATCC, Manassas, VA, USA) and cultured in RPMI-1640 cell culture medium supplemented with 10% fetal bovine serum (FBS). TBMS I of different concentration was diluted by RPMI-1640 without FBS. Cultured cells were maintained in a humidified incubator at 37°C in the presence of 5% CO_2. The culture medium was changed every 2 days. Cells for assay were serum starved for 24 h before being tested and harvested by detachment with a solution of 0.25% trypsin and 0.02% EDTA.

1.2 *In vitro* assay of cytoskeleton nanomechanics

The cytoskeleton nanomechanics were assayed by optical magnetic twisting cytometry (OMTC), a well established method for measuring nanomechanical properties of F-actin cytoskeleton. The details of the OMTC technique are described elsewhere [14,15]. In brief, cells (1×10^4 cells/well) were seeded in 96-well tissue culture plates which had been coated with collagen I (5 μg/mL) and cultured in RPMI-1640 growth medium supplemented with 10% fetal bovine serum for 24 h, then changed to serum-free RPMI-1640 for 24 h. Subsequently, serum-free RPMI-1640 medium was

Figure 1 The chemical structure of tubeimoside I.

changed, then added the RGD-coated magnetic beads onto cells and waited for 20 min to allow the beads to bind to receptors on the cell surface. Soon after, the dish was mounted onto a microscope stage custom fitted with the bead twisting setup. The beads were magnetized horizontally and then twisted in an oscillatory magnetic field. From the ratio of the applied magnetic torque to the measured lateral bead displacement, the complex elastic modulus was calculated and given as G', that is elastic modulus, or stiffness of the cytoskeleton, which has units of Pascal per nanometer as shown in Figure 2.

For measuring the cytoskeleton stiffness versus frequency, the cells were treated with either sham or TBMS I at 10, 20, 30 μmol/L, respectively, for 6 h. The F-actin stiffness was measured at frequency of 0.1, 0.3, 1, 5, 10, 30, 100 and 300 Hz, respectively, run by proprietary software.

For measuring the cytoskeleton stiffness versus time, the cell dish was mounted onto a microscope stage custom fitted with the bead twisting setup. The beads were magnetized horizontally and then twisted in an oscillatory magnetic field with a fixed frequency of 0.3 Hz, 60 cycles. Then 20 μL of 525 μmol/L TBMS I was quickly added into the cell dish and the cytoskeleton stiffness was continuously measured up to 5 min.

During each experiment, hundreds of cells with 171–556 beads were measured simultaneously for F-actin stiffness (G'). Values of G' measured by all the beads in one experiment were pooled together, and the median of the pooled G' was given as the cytoskeleton stiffness of each measurement. And for each experimental condition, the measurement of G' was repeated 6–10 times.

1.3   Structural assay of F-actin cytoskeleton

The structure of F-actin cytoskeleton was assayed by fluorescent microscopy. Cells (1×10^5 cells/well) were seeded on microscopic coverslips in the 96-well dish and then cultured in RPMI-1640 growth medium for 24 h. Thereafter the cells were treated with TBMS I at 10, 20, 30 μmol/L, respectively, for 24 h. Cells treated with sham containing equal volume of cell culture medium but no TBMS I (0 μmol/L) were used as control in every experiment throughout this study. Subsequently the buffer was removed, and then cells were fixed with 4% formaldehyde in PBS for 20 min at room temperature. After washing three times with 1.5 mL PBS, cells were permeabilized with 1.5 mL 0.1% Triton-X-100 in PBS for 5 min and subsequently blocked with 1.5 mL 1% BSA in PBS for 20 min. F-actin filaments were then stained with 80 μL FITC-phalloidin (1:40 dilution of 200 μg/mL stock in DMSO, Enzo Life Sciences, USA) for 20 min at room temperature. After staining, the cells were washed three times with 1.5 mL PBS. The stained cells were visualized with Leica TSP5 laser scanning confocal microscope (Leica Microsystems, Germany).

1.4   *In vitro* assay of cell migration

The migration activity of HepG2 cells was evaluated in vitro by using Transswell® chamber, a 24-well culture chamber with 8-μm pore size filter (Millipore, Billerica, MA). With each Transswell® chamber, the lower well was filled with RPMI-1640 cell culture medium containing TBMS I at either 0, 10, 20, or 30 μmol/L and supplemented with 20% fetal bovine serum. The upper well received 1×10^4 cells in 200 μL RPMI-1640 cell culture medium containing corresponding concentration of TBMS I (0, 10, 20, or 30 μmol/L, respectively). After incubation at 37°C for 8 h, cells remained on the upper side of the filter were considered non-migrating and were carefully eliminated with a cotton swab. Cells that had migrated across the filter to the lower well were collected and stained with 0.1% crystal violet (0.5 g crystal violet was dissolved by 100 mL methanol, then diluted with PBS of 4 times volume) for 30 min. The number of migrating cells collected from the lower well in each experiment was counted under optical microscope at 100× magnification. Results were expressed as the average
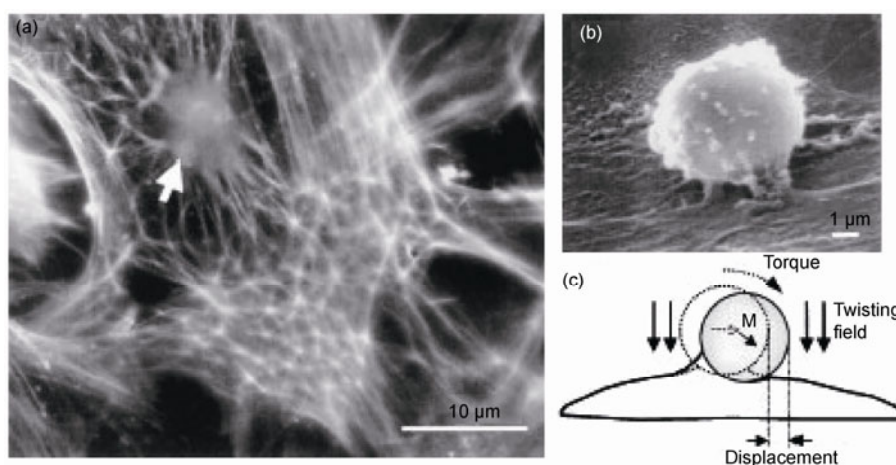
Figure 2   Illustration of optical magnetic twisting cytometry, as an *in vitro* assay of cytoskeleton nanomechanics.

number of migrating cells treated with TBMS I divided by the average number of migrating cells treated with sham.

1.5 Materials and reagents

Tubeimoside I was purchased from the National Institute for Control of Pharmaceutical and Biological Products (purity>98%, HPLC, Beijing, China). The 1 mmol/L stock solution of TBMS I was prepared in PBS and stored at −20°C. The stock solution was freshly diluted to the indicated concentrations with culture medium before use. Cell culture medium, RPMI-1640, and FBS were purchased from Biological Industries (Hyclone, USA), and Sijiqing Biological Engineering Materials Co., Ltd. (Hangzhou, China), collagen I was purchased from Nutacon BV (Netherlands), Magnetic beads were kindly provided as a gift by Professor Jeffrey J Fredberg of Harvard School of Public Health, Boston, MA. Synthetic Arg–Gly–Asp (RGD) sequence peptide was purchased from Peptite 2000 (Integra Life Sciences, Plainsboro Township, NJ, USA).

1.6 Statistical analysis

Except for the G' measurement, each experiment was repeated three times, and the result was presented as mean ± standard deviation (SD). The results obtained under different experimental conditions were evaluated using analysis of variance (ANOVA) followed by the Student's *t*-test, and differences were considered statistically significant when $P<0.05$.

2 Results

2.1 Cytoskeleton stiffness

The cytoskeleton stiffness of both the HepG2 cells and L-02 cells were influenced by TBMS I as shown in Figures 3 and 4, respectively. The effect of TBMS I was both frequency and time dependent. When measured at multiple frequencies, G' exhibited power-law behavior in all cases, that is G' increased in proportion to the power of measurement frequency, or $G' \propto f^{\alpha}$, where f is the frequency and α is the component of the power. However, the magnitude of G' and the value of α were dependent on the treatment of TBMS I. Specifically, both the magnitude of G' and the value of α appeared to decrease when the cells were treated with TBMS I at increasing concentration for both L-02 cells and HepG2 cells. As the concentration of TBMS I increased from 0, to 10, 20, and 30 μmol/L, the value of α for L-02 cells decreased from 0.1901, to 0.1285, 0.0933, and 0.0230, respectively (Figure 3(a)), while for HepG2 cells it decreased from 0.1983, to 0.1332, 0.0844, and 0.0145, respectively (Figure 3(b)).

When measured continuously at a fixed frequency but
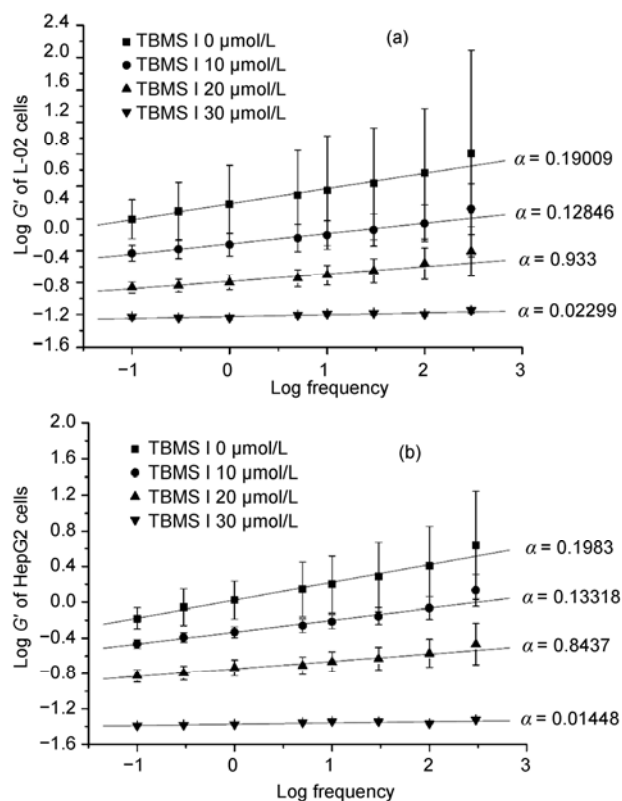
Figure 3 Relationship between measured G' and the loading frequency, f displayed as log G' vs. log f. (a) G' measured in L-02 cells; (b) G' measured in HepG2 cells. Symbols represent control condition (■, *n*=556), 10 μmol/L TBMS I (●, *n*=295), 20 μmol/L TBMS I (▲, *n*=239), and 30 μmol/L TBMS I (▼, *n*=171), respectively.

prior and post to addition of TBMS I to the cells, both HepG2 and L-02 cells responded to the addition of TBMS I by quickly loosing stiffness of the cytoskeleton (Figures 4 and 5). In HepG2 cells, the measured stiffness of the cytoskeleton was 0.44±0.01 Pa/nm prior to addition of TBMS I. Upon addition of 50 μmol/L TBMS I, the stiffness was
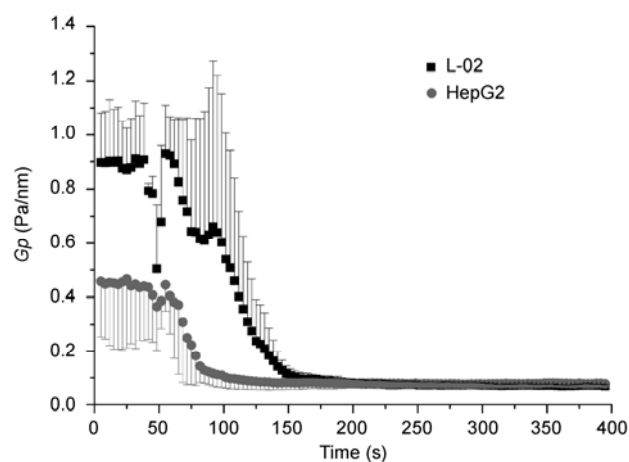
Figure 4 Time course of cytoskeleton stiffness in response to the addition of TBMS I. Symbols represent HepG2 cells, and L-02 cells, respectively (■, *n*=324; ●, *n*=196). TBMS I was added at 50 μmol/L.
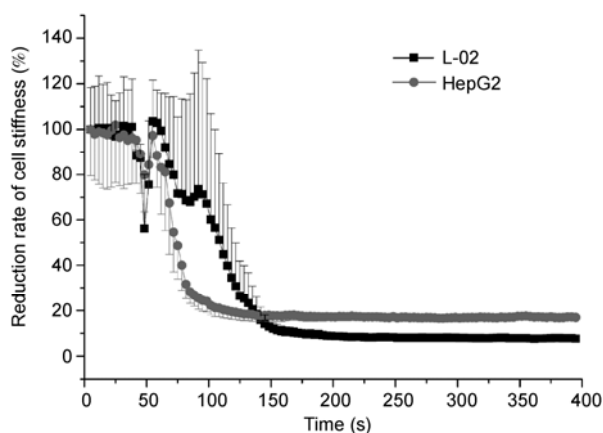
Figure 5 Normalized time course of cytoskeleton stiffness in response to the addition of TBMS I Symbols represent HepG2 cells, and L-02 cells, respectively (■, n=324; ●, n=196).

reduced to a minimal level (Figure 4). In L-02 cells, the stiffness (G') measured prior to addition of TBMS I was a high 0.88±0.04 Pa/nm, which also quickly reduced to almost floor upon addition of TBMS I (Figure 4).

Although both HepG2 and L-02 cells responded to TBMS I by reducing the cytoskeleton stiffness (G'), the speeds of their response were different. This difference is more obvious when the G' was all normalized to its initial value measured at the beginning of the experiment (Figure 5). It can be further demonstrated by the half time (T_{50}) that is the time when G' reduced to one half of its initial value between HepG2 and L-02 cells (73 vs. 109 s, P<0.05).

2.2 F-actin cytoskeleton

F-actin cytoskeleton of HepG2 cells appeared to be targeted by TBMS I. As shown in Figure 6(a), the HepG2 cells in the absence of TBMS I exhibited morphology of F-actin cytoskeleton that is normally seen with this type of cell. In contrast, in the presence of TBMS I, as the dose and exposure duration increased, the F-actin cytoskeleton in the cells appeared to be increasingly thin, irregularly shaped, and damaged along the edge of the cell. For example, after exposure to TBMS I for 24 h, the density of F-actin cytoskeleton in the cells treated with 10 μmol/L TBMS I appeared somewhat reduced with irregular shape as compared to control (Figure 6(b)), which was further reduced in cells treated with 20, and 30 μmol/L (Figure 6(c),(d)), indicating increasing depolymerization of F-actin in these cells.
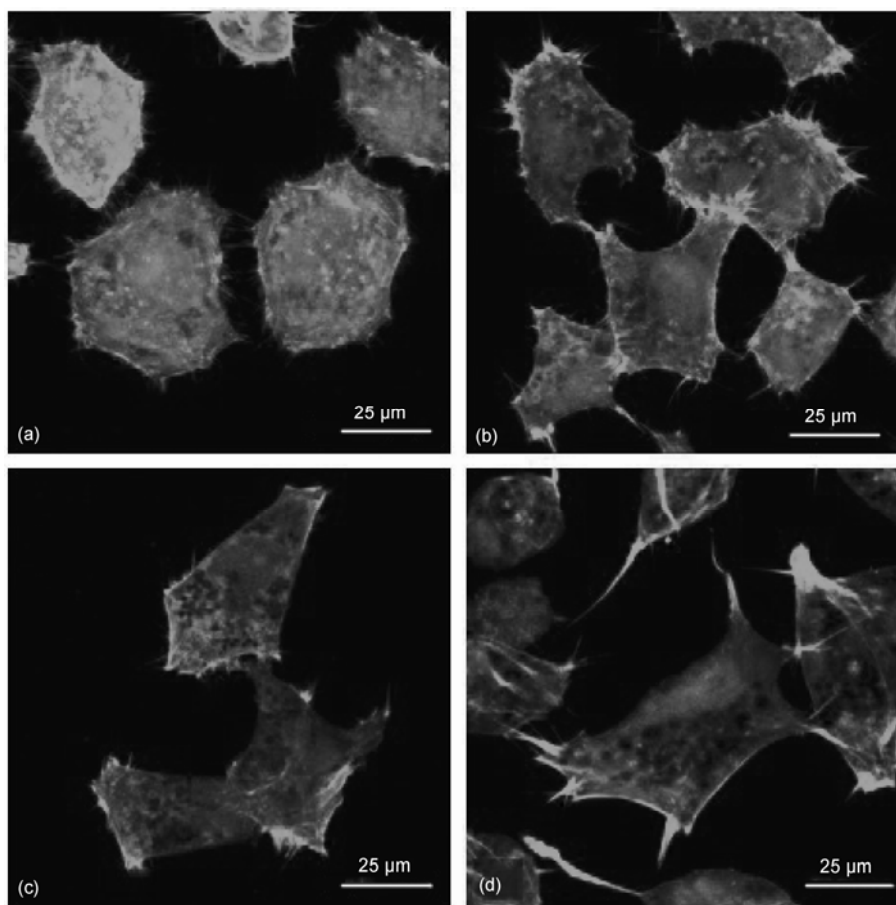
Figure 6 Structures of F-actin cytoskeleton of HepG2 cells imaged by using fluorescence confocal microscopy. Representative images of F-actin cytoskeleton treated by either sham (0 μmol/L) are shown in (a), or TBMS I at 10 μmol/L in (b), 20 μmol/L in (c), 30 μmol/L in (d) (100× mag.).

2.3   Cell migration

When HepG2 cells were treated with TBMS I for 8 h at increasing concentration (0, 10, 20 and 30 µmol/L), the cells became increasingly less able to migrate as demonstrated by fewer cells to have migrated through the filter of Transswell® chamber (Figure 7(a)–(d)). When compared to those treated with sham (the controls), the percentage of HepG2 cells that migrated through the filter of Transswell® chamber was 59.3% at 10 µmol/L, 29.6% at 20 µmol/L and 3.7% at 30 µmol/L, respectively (Figure 7(e)).

3   Discussion

The primary finding of this study is that exposure of HepG2 cells to TBMS I at increasing concentration increasingly reduced the cytoskeleton stiffness (G') and the value of exponent (α) for the power-law between the G' and the loading frequency ($G \sim f^{\alpha}$). In addition, while the F-actin cyto-skeleton of HepG2 cells appeared to be softer than that of L-02 cells in the absence of TBMS I, the F-actin cytoskeleton of HepG2 cells responded much quickly than that of L-02 cells to the stimulation of TBMS I. This was the first time that the cytoskeleton nanomechanics of a type of cancer cell, HepG2 cells was studied with respect to the anti-cancer effect of TBMS I as a potential drug candidate for cancer therapy.

In addition to cytoskeleton stiffness, TBMS I also inhibited migration of HepG2 cells. In parallel, the cells treated with TBMS I showed destruction and dissolution of the F-actin cytoskeleton labeled with FITC-Phalloidin. The results imply that TBMS I may target cancer cell's F-actin cytoskeleton and eventually alter the physical behaviors associated with F-actin cytoskeleton structure such as cancer cell invasiveness.

F-actin as a highly conservative protein, exists in the cytoplasm of all eukaryotic cells, and provides the primary structural component of the cytoskeleton. It is the most important determinant of cell mechanical properties/be-
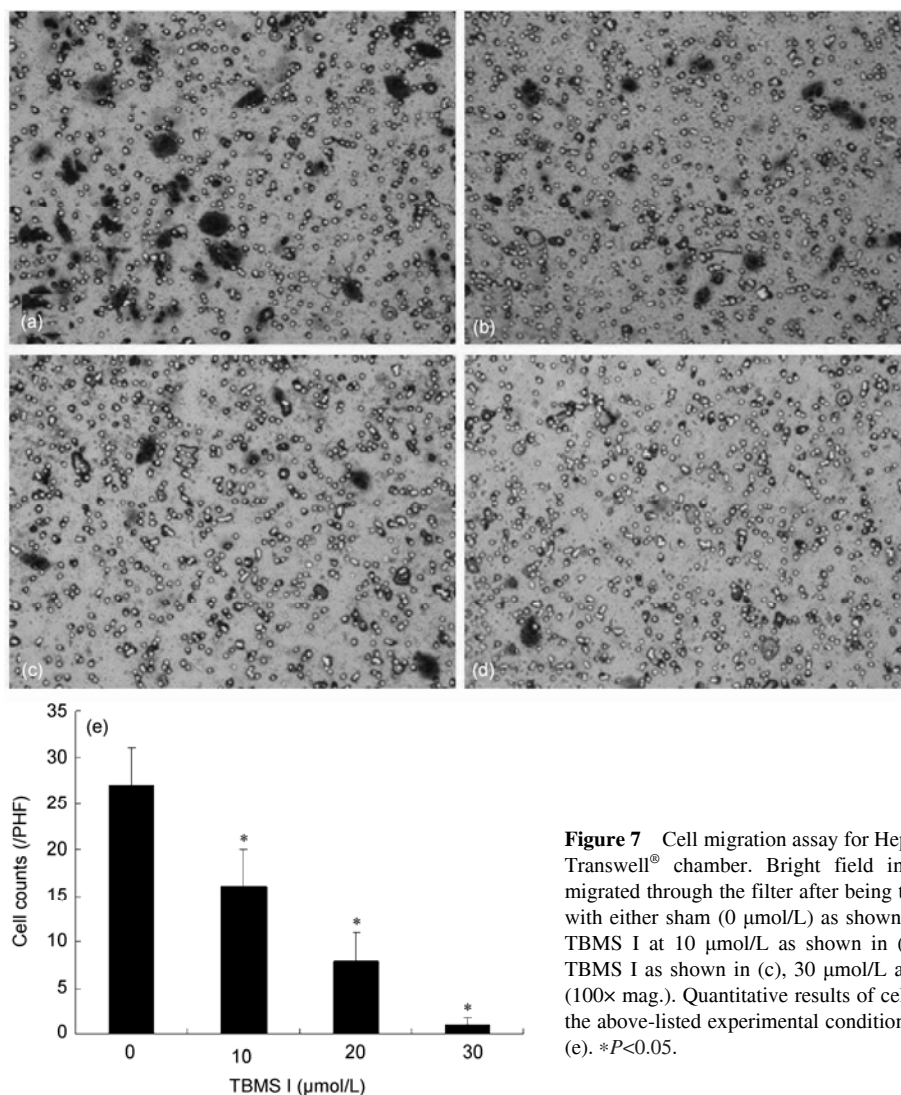
Figure 7   Cell migration assay for HepG2 cells using Transswell® chamber. Bright field images of cells migrated through the filter after being treated for 24 h with either sham (0 µmol/L) as shown in (a), or with TBMS I at 10 µmol/L as shown in (b), 20 µmol/L TBMS I as shown in (c), 30 µmol/L as shown in (d) (100× mag.). Quantitative results of cell migration for the above-listed experimental conditions are shown in (e). *$P<0.05$.

haviors. In response to extracellular signal stimulation, the F-actin cytoskeleton can change its structure and function rather swiftly via polymerization, depolymerization and rearrangement. It is now known that the F-actin cytoskeleton is not a static structure, instead, it is a very active and dynamic system. This system is constantly reorganizing itself in order to participate in and/or facilitate various important physiological activities such as division, migration, maintenance of cell shape and bearing external force [11–13].

Because RGD could bind to the F-actin cytoskeleton through the integrin receptor within the focal adhesions in the cell membrane, the stiffness measured by OMTC method directly reflects the mechanical properties of the F-actin cytoskeleton. OMTC employs magnetic manipulation and optical detection/quantification in an integrated system to allow a non-invasive method to assess the nanomechanics of cells. Using this method, hundred cells can be simultaneously assessed in one experiment. The fast response of cytoskeleton nanomechanics to drug agent is another advantage. These suggest that the method may have a great potential to be developed as a high throughput and rapid tool for drug screening.

The measured cytoskeleton stiffness of HepG2 and L-02 cells exhibited power-law behavior with regards the loading frequency, which is consistent with reports by Fabry et al. [16]. The value of exponent (α) for the power-law between the stiffness and the loading frequency ($G \sim f^{\alpha}$) reflects the state and tendency of fluidization for the cells. When $\alpha = 0$, it is pure solid; $\alpha = 1$, it is pure Newtonian fluid; $0 < \alpha < 1$, it is between solid and fluid, and at this time α determines the tendency of being solid or liquid [16]. The measured results show that the stiffness of HepG2 cells was smaller than that of L-02 cells in the absence of TBMS I. The value of α for HepG2 cells was, however, greater than that for L-02 cells. This suggests that the HepG2 cell is not only softer, but importantly more fluid-like than the L-02 cells. These nanomechanical behaviors are nevertheless consistent with the fact that the HepG2 cell is a cancer cell type that is characterized by greater ability to migrate and deform, all require the cells to be fluid. When TBMS I was in presence, both the stiffness and the value of α were reduced in all cases. The time course of measured G' also shows a prompt decline when TBMS I was added at a time point between 50 to 80 seconds. The degree of stiffness reduction in HepG2 cells was greater than that of L-02 cells. These results show that TBMS I may not only target F-actin cytoskeleton, but also selectively cause greater and faster changes of the F-actin cytoskeleton in cancerous cells such as HepG2 cells than in normal cells such as L-02 cells.

Changing mechanical properties of the cancer cells can also alter the cancer cells' interaction with their microenvironment, leading to either promotion or inhibition of cancer cell invasion and metastasis [17]. Therefore, it is necessary to elucidate the role of cancer cell cytoskeleton nanomechanics in regulating cancer cell growth and metastasis with or without anticancer drug intervention. Our finding that TBMS I caused destruction and dissolution of F-actin cytoskeleton, and corresponding decrease of the cytoskeleton stiffness and fluidity imply that cancer cells (HepG2) may be affected by anticancer drug (TBMS I) in a way to dysfunction in active motility and deformation. Thus, *in vitro* assay of the cytoskeleton nanomechanics of the cancer cells becomes necessary to properly reflect the pharmacological action of anticancer drug agent, TBMS I on the working of the F-actin cytoskeleton of HepG2 as a physical pathway to inhibit invasion and metastasis of the cancer cells. This pathway is an important supplement to the molecular pathways of TBMS I in HepG2 cells including apoptosis as reported by Wang et al. [18,19].

It should be noted that the present study is limited to cells from one cancer type. Cells from other types of cancer including breast cancer, lung cancer and pancreas cancer have been examined for their nanomechanics by different techniques such as atomic force microscopy [20,21]. The results reported by those studies are, in general, consistent with our findings despite the differences in cancer types and measurement methods employed. Nevertheless, it is indeed necessary to further test other cancer types in regards their nanomechanics response to the administration of anticancer drug. In addition, it is likely that the anticancer drug such as TBMS I targets cytoskeleton nanomechanics via multiple pathways apart from the F-actin structure. For instance, the myosin light chain (MLC) in cancer cells may well be affected by anticancer drug, which would change the state of intracellular tension and ultimately contribute to altering cytoskeleton nanomechanics. Further studies are required to fully elucidate the mechanisms that mediate the drug-induced changes in cytoskeleton nanomechanics.

Taken together, we conclude that *in vitro* assay of cytoskeleton nanomechanics could be used as a novel tool in drug screening in addition to other conventional tools. Using this method, we confirmed that TBMS I was a potent agent to target cytoskeleton stiffness and fluidization of hepatoma (HepG2) cells. The pharmacological effects were mediated by suppression of the cells' motility via dismantling the F-actin cytoskeleton structure. Furthermore, the difference in response speed of cytoskeleton stiffness between HepG2 cells and L-02 cells, to the stimulation of TBMS I, suggests a certain specificity of targeting cytoskeleton nanomechanics by the anticancer drug. This was a novel finding of the role of TBMS I in regulation of cancer cell structure and function, providing a supplemental mechanism of cytotoxicity and drug sensitivity for TBMS I. Considering its preferential distribution in the liver and its origin of natural medicinal plant, this study suggests that TBMS I may be a useful drug candidate for treating liver cancer.

1   Zhao X. Supplement to the Compendium of Materia Medica, Reprinted from the 1765 Wood-engraved Edition in Chinese Language. Beijing: The People's Medical Publishing House, 1983. 123

2   Yu L, Ma R, Wang Y, et al. Potent anti-tumor activity and low toxicity of tubeimoside I isolated from Bolbostemma Paniculatum. Planta Med, 1994, 60: 204–208

3   Wang Y, Yu L, Zhu J, et al. Studies on antitumor action of extracts of Bolbostemma Paniculatum (Maxim.) Franquet. J Shaanxi Med, 1981, 10: 55–59

4   Kong F, Zhu D, Xu R, et al. Structural study of tubeimoside I, a constituent of Tu-Bei-Mu. Tetrahedron Lett, 1986, 27: 5765–5775

5   Hu Z, Ma R D, Yu L J. Effects of tubeimoside I on cell cycle and apoptosis of human myeloblastic leukemia cells (Hl-60). Chin J Clin Oncol, 2003, 30: 163–171

6   Ma R D, Weng X Y, Yu L J, et al. Apoptosis of human nasopharyngeal carcinoma CNE-2Z cell line induced by tubeimoside I isolated from Bolbostemma Paniculatum. Chin J Cancer, 2003, 22: 806–811

7   Ma R D, Yu L J, Su W M, et al. Induction of cell cycle arrest and apoptosis by tubeimoside I isolated from Bolbostemma Paniculatum in Hela cells. Chin J Clin Pharmacol Ther, 2004, 9: 261–269

8   Ma R, Song G, You W, et al. Anti-microtubule activity of tubeimoside I and its colchicine binding site of tubulin. Cancer Chemother Pharmacol, 2008, 62: 559–568

9   Wang F, Ma R D, Yu L J. Role of mitochondria and mitochondrial cytochrome C in tubeimoside I-mediated apoptosis of human cervical carcinoma HeLa cell line. Cancer Chemother Pharmacol, 2006, 57: 389–399

10 Xu Y, Chiu L F, He Q Y, et al. Tubeimoside-I exerts cytotoxicity in Hela cells through mitochondrial dysfunction and endoplasmic reticulum stress pathways. J Proteome Res, 2009, 8: 1585–1593

11 Lazarides E, Weber K. Actin antibody: The specific visualization of actin filaments in non-muscle cells. Proc Natl Acad Sci USA, 1974, 71: 2268–2272

12 Durham J T, Herman I M. Inhibition of angiogenesis *in vitro*: A central role for beta-actin dependent cytoskeletal remodeling. Microvasc Res, 2009, 77: 281–288

13 Rando O J, Zhao K, Crabtree G R. Searching for a function for nuclear actin. Trends Cell Biol, 2000, 10: 92–97

14 Fabry B, Maksym G N, Butler J P, et al. Scaling the microrheology of living cells. Phys Rev Lett, 2001, 87: 148102

15 Fabry B, Maksym G N, Butler J P, et al. Time scale and other invariants of integrative mechanical behavior in living cells. Phys Rev E Stat Nonlin Soft Mat Phys, 68: 041914

16 Fabry B, Maksym G N, Shore S A, et al. Selected contribution: Time course and heterogeneity of contractile responses in cultured human airway smooth muscle cells. J Appl Physiol, 2001, 91: 986–994

17 He H B, Tang X F. Advances in biomechanics research of cancer cells. Foreign Med Sci Stomotol, 2004, 31: 273–275

18 Wang Y, Deng L, Zhong H, et al. Natural plant extract tubeimoside I promotes apoptosis-mediated cell death in cultured human hepatoma (HepG2) cells. Biol Pharm Bull, 2011, 34: 831–838

19 Wang Y, Deng L, Wang Y, et al. Natural plant extract tubeimoside I induces cytotoxicity via the mitochondrial pathway in human normal liver cells. Mol Med Reports, 2011, 4: 713–718

20 Chen P P, Dong H T, Chen L, et al. Application of atomic force microscopy to living samples from cells to fresh tissues. Chin Sci Bull, 2009, 54: 2410–2415

21 Cross S E, Jin Y, Rao J, et al. Nanomechanical analysis of cells from cancer patients. Nat Nanotechnol, 2007, 2: 780–783